Near-infrared fundus camera based on polarization switch in stray light elimination

Haishui Ye (叶海水), Zhishan Gao (高志山)*, Zhenyu Qin (秦震宇), and Qianwen Wang (王倩雯)

School of Electronic and Optoelectronic Technology, University of Science and Technology, Nanjing 210094, China

**Corresponding author: zhishgao@mail.njust.edu.cn*

Received September 18, 2012; accepted November 16, 2012; posted online February 28, 2013

This letter shows that the human eye fundus tissue has higher reflectivity at the near-infrared (NIR) wavelength, and that some aberrations exist at the pre-optical system from cornea to vitreous. We design a NIR fundus camera with inner focusing, which can be applied to the –10 D to 10 D range of vision and has the advantage of ensuring the stability of image when is focused. Considered as Liou's eye aberration model, we correct the integrated aberration to ensure a 100 lp/mm resolution when we complete the assembly and calibration of the fundus camera. Kohler illumination is also applied to obtain uniform fundus illumination. Moreover, we put forward a novel method for stray light elimination based on polarization switch, which inhibits ghost image formation near the focal plane when the illumination beam is reflected by the eyepiece surface. The result shows that this method is effective in ensuring an illumination uniformity of 80%, with the advantage of simple structure and easy assembly.

OCIS codes: 170.0110, 260.5430, 220.2945.

doi: 10.3788/COL201311.031702.

A fundus camera is an optical system that directly images retinal tissue, which can be used in fields such as ophthalmic clinical medical diagnosis. Compared with a common imaging system, a fundus camera has a special illumination path to achieve a uniform illumination of the fundus tissue, thus complementing the illumination insufficiency of the imaging optical paths caused by the low reflectivity of fundus tissue[1]. The German company Zeiss produces fundus cameras with halogen lighting. Delori *et al.* have shown that human retinal tissue reflectivity is maintained at around 1% to 10% in the visible and near-infrared (NIR) bands[2]. The NIR 800-nm band reflectivity is maintained at the highest value of 10%; thus, this band is chosen as the working band of the proposed fundus camera.

The effect of stray light on image quality should be considered in the design of the fundus camera because of the human eye's complex structure, which mainly includes two aspects: one is the stray light reflected by the corneal surface and the other is the ghost image of the eyepiece in the common optical path. Cornea has higher reflectivity at the NIR wavelength, thus high brightness of background may result in imaging retinal tissue with lower reflectivity. Therefore, controlling corneal reflected light is crucial in designing the fundus illumination path. The fundus imaging system[3] introduces a special annular Kohler illumination, in which, the illumination beam enters the intraocular medium from the pupil edge and the beam is reflected by the fundus tissue exits from the pupil center. The corneal reflection distribution to the illumination beam shows that the reflected intensity in the center is stronger than that at the edge, whereas the annular Kohler illumination can effectively avoid higher corneal reflection to improve the contrast of the fundus image. Controlling the amount of light incident to the fundus within the security exposure dosage range is necessary. Taking into account the human eye's comfort under NIR light, uniform illumination is also required when designing the illumination path[4].

The imaging optical path should be an adjustable focal length that can be applied to the fundus with different diopters, and is partially similar to the illumination path, which mainly refers to the eyepiece and the human eye. The intrinsically low reflectivity of the fundus tissue determines the strong noise caused by the ghost image formed near the imaging system focal plane when the illumination beam is reflected by the eyepiece surface. A traditional method to eliminate ghost image is to add black dot boards[5−7] in the illumination path, that is, making the ghost image analysis specific to the eyepiece components and adding black dot boards to block ghost images entering the imaging path, thereby inhibiting ghost image formation at the focal plane to improve the signal-to-noise ratio (SNR). This method effectively blocks the ghost image, but each reflection surface of the eyepiece component needs a black spot board; its position and dot size must be strictly controlled as well. For an eyepiece group with a number of pieces, increasing the black spot boards leads to difficulty in mechanical structure, assembly, and calibration, as well as to an increase in optical energy loss, which affects illumination energy utilization efficiency. Imaging path focusing techniques include moving the eyepiece[8], imaging objective lens or charge-coupled device (CCD)[9], two deflection-angle prism method[10], and inner focusing[11]. Moving the eyepiece easily leads to position change of the pupil conjugate image, resulting in failure of Kohler illumination and changes in the position of the black dot board. Therefore, additional auxiliary optical arrangements are needed to adjust the black dot boards.

Based on previous fundus camera designing results with inner focusing structure, this letter carries conducts NIR fundus camera assembly and stray light reduction. In this process, we put forward a method for stray light elimination based on the polarization switch technique, inhibiting the ghost image caused by the eyepiece in the common path of imaging and illumination optical path. This method has the advantages of simple structure and convenient installation.

In the common optical path of a fundus camera, the eyepiece generally uses ocular structure, namely, short focal length with large field and relatively large $F/\#$. For convenience, the exit pupil distance of the eyepiece should be above 20 mm and the exit pupil diameter should be maintained within 2–4 mm. The characteristics of the focusing lens and objective lens must be synthetically considered to determine the eyepiece surface type and curvature. The imaging path realizes the focusing process with inner focusing structure. Combined with a human eye aberration model, symmetric structure was used to design the eyepiece and the focusing lens. The objective lens contributes more to aberration with multi-piece and complex structure lens.

The stray light that the CCD receives comes from two main sources: reflected light from the cornea and reflected light from each eyepiece surface. With an annular aperture incident from the corneal margin, corneal reflected light can be emitted from the imaging path, thereby avoiding its involvement in imaging. The system design uses coaxial illumination, in which imaging and illumination paths share the same eyepiece group, indicating that the surface reflected light also goes into the imaging path and is received by CCD to form a ghost image. The existence of ghost images will decrease the image SNR, thus black dot boards should be added in the illumination path to eliminate ghost images.

The ghost image analysis method involves taking the aperture stop of an imaging path as the object of the eyepiece, changing the eyepiece surface to be analyzed from the original refracting surface to the reflecting surface while other optical surfaces remain as refracting surfaces, and then reverse tracing rays in ZEMAX to obtain the ghost image position and size. We calculated the each ghost image that corresponds to the eyepiece rest surfaces; the results are shown in Table 1.

The ghost image position in Table 1 takes the last surface of eyepiece for reference. The black dot size should entirely cover and be slightly greater than the ghost image. From the data in Table 1, the distance between the black dot boards of surface 2 and surface 5 is only 0.2 mm, thus they merely need to share a piece of black dot board located at the position 75.8 mm after the eyepiece's last surface; its size is 1.0 mm. Five pieces of black dot boards should be added into the illumination path to eliminate the ghost image formed by the eyepiece surface.

When the ghost image with black dot board is eliminated, the illumination arrangement will become more complex. Fabrication and accurate calibration of the black dot board enhance the difficulty in system assembly. Increasing the number of black spot boards also increases the energy loss to a certain extent.

Table 1. Position and Size of Ghost Image (mm)

Surface	1	2	3	4	5	6
Radius	–174.14	12.50	–15.31	15.31	–12.50	174.14
Thickness	1.5	5.4	0.08	5.4	1.5	—
Ghost Position	68.3	75.8	78.9	73.0	75.6	93.43
Black Spot Size	1.4	0.8	1.0	0.8	0.8	1.4

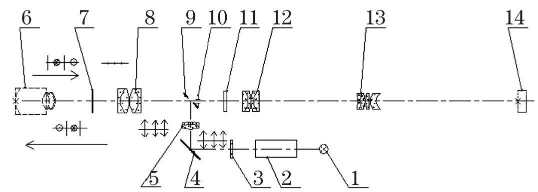

Fig. 1. Fundus camera with a polarization switch. 1: light source, 2: uniform light system, 3: polarizer slice, 4: reflector, 5: condenser lens, 6: human eye model, 7: quarter-wave plate, 8: eyepiece, 9: hollow mirror, 10: aperture stop, 11:analyzer slice, 12: focusing lens, 13: objective lens, and 14: CCD.

Based on the principle that linear polarization components are sensitive to polarization state, the polarization switch allows the propagation of polarization beams with the same direction as its light vector while blocking polarization beams perpendicular to its light vector, thereby fulfilling the "switch" function of the optical path. In this study, the design of a fundus camera employs polarization switch principle to block the optical path of stray light. The system structure is shown in Fig. 1.

NIR fundus camera based on polarization switch includes two parts: imaging path and illumination path. The illumination path uses the folding optical path technique to maintain the advantages of compact mechanical structure; thus, a reflector is added to the illumination path after the hollow mirror and condenser lens to transfer illumination beams exiting from the light source, uniform light system, and polarizer slice to the common path. The light source adopts NIR superluminescent diode with a central wavelength of 830 nm, and the CCD uses Clara series (pixels $1\,392\times1\,040$) produced by Andor Corporation. Polarization switches consisting of polarizer slice, analyzer slice, and quarter-wave plate were applied to the illumination and imaging paths. Assuming that the light vector direction of the polarizer slice is the same as the optical axis, the emergent illumination beam also has the same polarization state, with Jones vector $\mathbf{S}_0 = [1\ 0]^{\mathrm{T}}$. A 45° angle exists between the quarter-wave plate's fast axis and optical axis. The Jones vector formula of the illumination beam incident to the fundus tissue is expressed as

$$\mathbf{S}_1 = \mathbf{J}_{\mathrm{q}}\mathbf{S}_0, \tag{1}$$

$$\mathbf{J}_{\mathrm{q}} = \frac{1}{\sqrt{2}}\begin{bmatrix} 1 & -\mathrm{i} \\ -\mathrm{i} & 1 \end{bmatrix}. \tag{2}$$

As Eq. (1) shown, the Jones vector of the fundus tissue's illumination beam is $1/\sqrt{2}[1\ -\mathrm{i}]^{\mathrm{T}}$, i.e., right rotation circularly polarized the light shown in Fig. 1. The illumination beam reflected by the fundus tissue again goes through the quarter-wave plate. The emergent beam vector is shown as Eq. (1), i.e., $[0\ 1]^{\mathrm{T}}$. Similar to the linearly polarized light, its light vector direction is perpendicular to the optical axis and the polarization state of ghost image formed by each reflection surface of the eyepiece. As long as the light vector direction of the analyzer slice is perpendicular to the optical axis, simultaneously allowing the fundus reflex light to go through the analyzer slice and blocking the ghost image into the CCD is possible, thereby eliminating stray light, such as ghost image. The

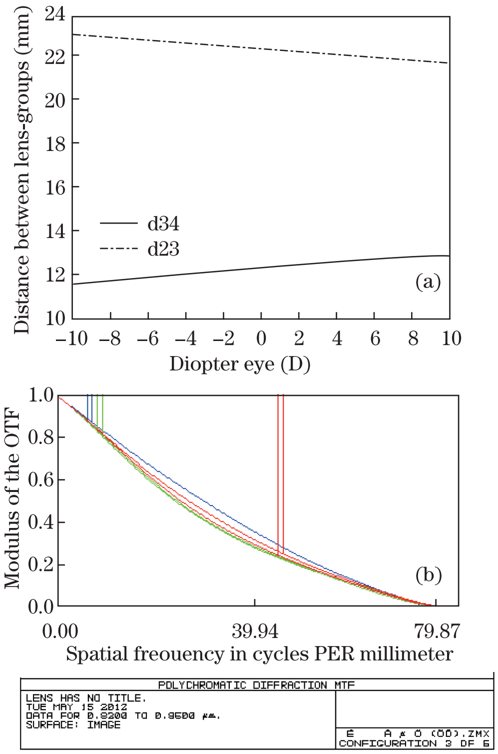

Fig. 2. (a) Focusing curve and (b) MTF curve.

Table 2. System Parameters of the Fundus Camera

Field of View (FOV)	4°
Magnification (emmetropia)	2.5
Entrance Pupil Diameter (mm)	2.5
Resolution (lp/mm)	74
Depth of Field (μm)	118.8
Focusing Range	–10 D to 10 D
Illumination Uniformity	> 80%

insertion of a wave plate increases energy loss merely due to its surface-coating performance. The phase delay aroused by the wave plate will not contribute to energy loss. When natural light goes through the polarizer slice, half of the energy will be lost.

Based on Liou's eye aberration model, we designed a NIR fundus camera with inner focusing. The focusing curve linearly changes, as shown in Fig. 2(a). In emmetropia cases, the cut-off frequency of the MTF curve is 74 lp/mm, as shown in Fig. 2(b).

The system parameters of the fundus camera, such as field of vision, magnification, resolution, and focusing range, are shown in Table 2. The depth of field is specific to this case, which belongs to long depth of field design.

Fundus illumination uses Kohler illumination for the design, where the light source and the fundus form conjugate imaging pairs. As shown in Fig. 3(a), we used ASAP software (BRO. Inc) to analyze the uniformity of the illumination path, and obtain the fundus illumination results shown in Fig. 3(b) by establishing a mathematical model of fundus illumination path in the software and using 10 million rays for ray tracing. The illumination area is circular, with a radius greater than 3 mm, covering the field of view (FOV) range of the fundus imaging optical path.

The distribution of fundus luminous flux is more concentrated in the central area than at the edge, and the illumination uniformity is better than 80% in the illumination area with a diameter of 2 mm. As shown in Fig. 4, we used the polarization switch technique to eliminate ghost image, i.e., mounting a quarter-wave plate between the eyepiece and the human eye model, with the polarizer and analyzer slices arranged behind the light source or between the focusing lens and the hollow mirror.

In the experiment, we used human a eye model as the object to test the system performance. We made an optical component with the same refractive capacity as the human eye and replaced the retina of the human eye with the resolution test pattern. Figure 5(a) shows the test result of the imaging path performance. The 23rd line pair of shot N4 resolution test pattern (matched component of F1300 parallel light pipe, Xiaogan Huazhong Photoelectric Instrument Co., Ltd.) was clearly visible, and the resolution of the imaging path was 100 lp/mm. The corneal surface illumination result is shown in Fig. 5(b). Elliptic annular uniform illumination ensures its separation from the imaging path and prevents reflected light from entering the imaging path.

The ghost image elimination process is described as follows. Before the installation of the quarter-wave plate, the analyzer slice was rotated to achieve the best extinction. The light vector directions of the

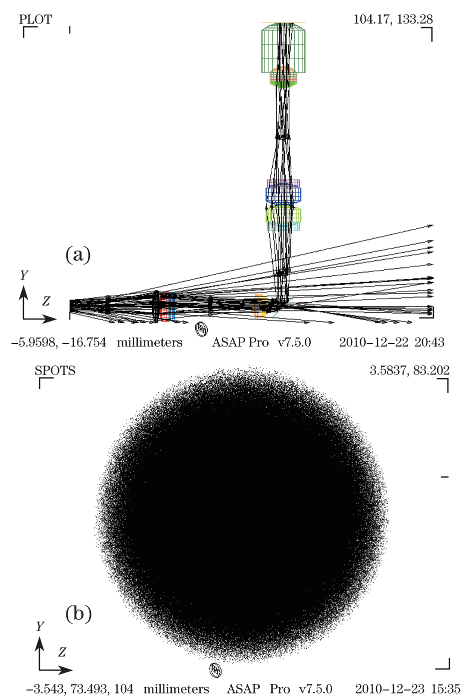

Fig. 3. Simulation result in ASAP. (a) Ray tracing; (b) illumination distribution.

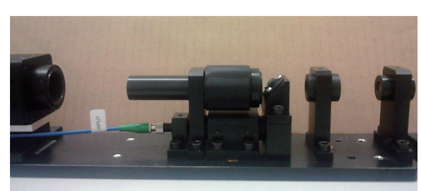

Fig. 4. Fundus camera arrangement.

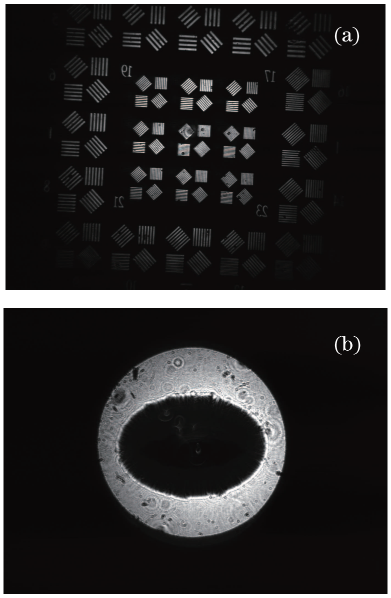

Fig. 5. (a) N4 resolution test pattern image and (b) elliptic annular illumination.

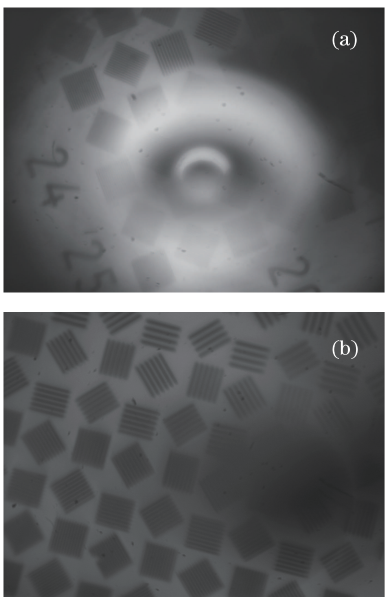

Fig. 6. Ghost images (a) before and (b) after elimination.

polarizer and analyzer slices are perpendicular to each other, blocking the ghost image into the imaging path. The quarter-wave plate is then installed and rotated; thus the included angle between its fast axis and the analyzer remains at 45°. The beam reflected by the resolution test pattern undergoes the polarization state conversion from linear to circular to linear again, which is the same as the light vector direction of the analyzer. Finally, it images on the CCD target surface. As shown in Fig. 6(a), ghost image interference exists near the focal plane of the imaging path, and the resolution test pattern image in Fig. 6(b) eliminates these ghost image effects.

A NIR fundus camera with inner focusing can obtain clear images of the fundus tissue with different diopters. The fundus camera presented in this study corrects the human eye's integrated aberration in a small field range, which can be applied to the −10 D to 10 D range of vision, and has high resolution. The fundus camera has a compact structure, with a total length of less than 300 mm. The hollow mirror connects the imaging path to the illumination path, and the latter uses the reflection type structure to reduce the height of the camera.

In conclusion, the illumination path design uses Kohler illumination to ensure fundus illumination uniformity better than 80%. We use the polarization switch technique to eliminate the eyepiece's ghost image. The experiment result shows that this method can effectively block ghost images from the imaging path, improve the extinction ratio of the polarizer and analyzer, and precisely control their light vector directions perpendicular to each other and the quarter-wave plate's fast axis at an included angle of 45°, all of which can further reduce the ghost image. In the experiment, we use the polarizer and the analyzer with extinction ratio of 500:1; however, some residual interference remains, as shown in Fig. 6(b). Thus, we recommend using a polarizer and an analyzer with extinction a ratio of 10 000:1.

This work was supported by the National Natural Science Foundation of China (Nos. 60977008 and 60678048), the National Ministry Education Fund for Doctoral of China (No. 20103219110014), and the Chinese Academy of Sciences Key Laboratory Fund (No. 2008DP173445).

References

1. M. Hammer and D. Schweitzer, Phys. Med. Biol. **47,** 179 (2002).
2. F. C. Delori and K. P. Pflibsen, Appl. Opt. **28,** 1061 (1989).
3. E. DeHoog and J. Schwiegerling, Appl. Opt. **47,** 6769 (2008).
4. E. DeHoog and J. Schwiegerling, Appl. Opt. **48,** 221 (2009).
5. N. Kishida and S. Ono, "Eye fundus examination apparatus" US Patent 7055955 (2006).
6. N. Ichikawa and S. Ono, "Fundus camera" US Patent 7219996 (2007).
7. C. Li, Q. Sun, Y. Liu, Q. Lu, J. Wang, J. Sun, J. Liu, and F. Qu, Chin. J. Opt. Appl. Opt. (in Chinese) **3,** 363 (2010).
8. Z. Wang and Y. Xu, Opt. Precis. Eng. (in Chinese) **16,** 1567 (2008).
9. Y. Xu, Z. Wang, and Y. Tian, Acta Photon. Sin. (in Chinese) **38,** 1122 (2009) .
10. Y. Zhang, G. Zhao, X. Zhang, and Y. Gu, Opt. Precis. Eng. (in Chinese) **17,** 1014 (2009).
11. H. Ye, Z. Gao, T. Luo, and Y. Huang, Chin. Opt. Lett. **8,** 689 (2010).